



Long-term (1749–2015) Variations of Solar UV Spectral Indices

Francesco Berrilli¹ · Serena Criscuoli² ·
Valentina Penza¹ · Mija Lovric¹

Received: 19 August 2019 / Accepted: 25 February 2020 / Published online: 9 March 2020
© Springer Nature B.V. 2020

Abstract Solar radiation variability spans a wide range in time, ranging from seconds to decadal and longer. The nearly 40 years of measurements of solar irradiance from space established that the total solar irradiance varies by $\approx 0.1\%$ in phase with the Sun's magnetic cycle. Specific intervals of the solar spectrum, e.g., ultraviolet (UV), vary by orders of magnitude more. These variations can affect the Earth's climate in a complex non-linear way. Specifically, some of the processes of interaction between solar UV radiation and the Earth's atmosphere involve threshold processes and do not require a detailed reconstruction of the solar spectrum. For this reason a spectral UV index based on the (FUV-MUV) color has been recently introduced. This color is calculated using *SORCE SOLSTICE* integrated fluxes in the FUV and MUV bands. We present in this work the reconstructions of the solar (FUV-MUV) color and Ca II K and Mg II indices, from 1749–2015, using a semi-empirical approach based on the reconstruction of the area coverage of different solar magnetic features, i.e., sunspot, faculae and network. We remark that our results are in noteworthy agreement with latest solar UV proxy reconstructions that exploit more sophisticated techniques requiring historical full-disk observations. This makes us confident that our technique can represent an alternative approach which can complement classical solar reconstruction efforts. Moreover, this technique, based on broad-band observations, can be

This article belongs to the Topical Collection:
Irradiance Variations of the Sun and Sun-like Stars
Guest Editors: Greg Kopp and Alexander Shapiro

✉ F. Berrilli
francesco.berrilli@roma2.infn.it

S. Criscuoli
scriscuo@nso.edu

V. Penza
valentina.penza@roma2.infn.it

M. Lovric
mija.lovric@roma2.infn.it

¹ Physics Department, University of Rome Tor Vergata, Via Ricerca Scientifica, 1, 00133, Rome, Italy

² National Solar Observatory, 3665 Discovery Dr., Boulder, CO 80303, USA

utilized to estimate the activity on Sun-like stars, that cannot be resolved spatially, hosting extra-solar planetary systems.

Keywords Sun: activity · Sun: UV radiation · Sun: faculae, plages

1. Introduction

Solar radiation changes over different temporal scales, with amplitudes that strongly depend on the spectral range considered. These variations can affect the Earth's climate in a complex way, and over temporal scales that vary from weeks to centuries, depending on the specific feedback considered (Lean, 2017). To address the impact that solar radiation has on the Earth's climate, it is therefore critical to be able to estimate variations of the solar spectral energy distribution over different temporal scales, that span from decadal to centennial and longer (Jungclaus *et al.*, 2017). For this reason, various and sophisticated models of total and spectral solar irradiance (TSI and SSI) variability have been produced which aim to reconstruct solar irradiance in the past (e.g., Yeo, Krivova, and Solanki, 2017, and references therein).

Particularly, the solar UV radiative output is strongly dependent on the phase of the Solar Cycle and is a relevant factor to our understanding of the Earth's climate dynamics. Notably, stratospheric ozone, which might influence the thermal and dynamical structure of the middle terrestrial atmosphere and consequently the radiative forcing of the troposphere (Haigh, 2003), is produced by the action of solar UV radiation on diatomic oxygen. Indeed, this radiation has enough energy to dissociate molecular oxygen and activate the photochemical cycle able to create and break down stratospheric ozone, playing a central role in the thermal structure of Earth's high atmosphere. The ozone production/destruction process (Chapman, 1932) involves six different reactions. In particular, the two photochemical processes that lead to the dissociation of molecular oxygen and ozone require the presence of UV photons at two different thresholds: 100–200 nm and 200–300 nm for the dissociation of oxygen and ozone, respectively.¹ As a consequence, the threshold processes associated with solar UV, for which the detail of the solar spectrum can be neglected in the first approximation, are the main responsible for defining stratospheric ozone production rates and column densities e.g. Bordi, Berrilli, and Pietropaolo, 2015). Recent works, (e.g. Seppälä *et al.*, 2014), indicate that a correct assessment of the impact of UV variability on global circulation requires the detailed knowledge of the column stratospheric ozone, as a main driver in the so-called top-down mechanisms. In the case of the Earth's climate, the abundance of ozone must be modeled in the past if we want to study the effects, global or regional, of the modulation of solar UV radiation. This also applies if one wants to use 3D Global Circulation Models to simulate the climate of exoplanets, obviously under simplified conditions of similarity in the behavior of the host-star with our Sun and Earth-like atmospheres. Similarly, indeed, UV radiation drives photochemical processes of exoplanet atmospheres (e.g. Linsky, 2014, 2017) and is co-responsible of their atmospheric mass-loss. The UV spectrum of the hosting star, and its variability, are therefore fundamental to properly characterize the atmosphere and determine the habitability of exoplanets (e.g. Tian *et al.*, 2014; Kaltenegger, 2017).

¹Actually, a correct determination of the ozone concentration with the atmospheric altitude based on the Chapman theory alone cannot explain the observed distribution of ozone. A detailed calculation requires the inclusion of the rates of photochemical reactions with temperature, a radiative transfer model for terrestrial atmosphere, and the NO_x catalytic cycles modulated by solar magnetic activity via solar energetic particles and cosmic rays modulation.

With the aim of studying the dependence of terrestrial total column stratospheric ozone on changes in solar UV spectral slope and possibly extending this approach, albeit under simplified assumptions, in the behavior of Sun-like stars, we introduced a spectral UV index based on the (FUV-MUV) color (Lovric *et al.*, 2017; Criscuoli *et al.*, 2018) in order to directly connect the variability of the solar UV spectral slope with solar activity indices. This color is calculated using Solar Radiation and Climate Experiment (SORCE) Solar Stellar Irradiance Comparison Experiment (SOLSTICE) integrated fluxes in the solar far UV (FUV) and solar middle UV (MUV) bands. The adopted (FUV-MUV) color is selected on the basis of its sensitivity to the ratio between solar UV contribution from the lower chromosphere and photospheric continuum. Indeed, as reported in Lean (1987), the solar UV contribution between 120–200 nm is primarily a continuum emission from the upper photosphere and lower chromosphere, with superimposed chromospheric emission lines and some absorption lines, while longward of 200 nm the spectrum is largely photospheric continuum radiation, with a collection of superimposed absorption lines.

Indeed, the UV radiative flux shows clear positive correlation with the magnetic activity of the stars, so that it is widely used as proxy of the magnetic field, when direct measurements are not available. In this respect, the Mg II H and K (280 nm) and Ca II K and H lines (393 and 396 nm) are excellent proxies, as their cores, that form at similar heights in stellar chromosphere, go into strong emission in the presence of magnetic fields (e.g. Linsky, 2017). The Mg II line is not accessible with ground observations and it has been monitored only since the late-1970s. Solar observations of the Ca II line started instead at the beginning of the 19th century and have continued with various programs, which included the acquisition of spectro-heliograms, full-disk broad-band observations (e.g. Bertello *et al.*, 2016; Chatzistergos *et al.*, 2019) and Sun-as-a-star observations. Being one of the widest lines in the solar spectrum, observations at different positions within the line allow to observe a broad range of the solar atmosphere (Ermolli *et al.*, 2010). Ca II K and Mg II observations provide the most widely used proxies for facular contribution in irradiance reconstruction models (e.g. Fontenla *et al.*, 2011; Lean, 2000) and can be used for studies of long-term evolution of the magnetic field (e.g. Pevtsov *et al.*, 2016; Chatterjee *et al.*, 2019). Monitoring of bright dwarf stars in this spectral range was started at Mount Wilson in 1968 (Wilson, 1978) and was continued by the Solar Stellar Spectrograph (SSS) at the Lowell Observatory starting 1994 (e.g. Hall and Lockwood, 1998). Such observations have been employed in various studies to characterize stellar magnetic activity, constrain stellar dynamo models and characterize solar activity in a more general context (e.g. Saar and Brandenburg, 1999; Böhm-Vitense, 2007; Egeland *et al.*, 2017; Warnecke, 2018).

The work is structured as follows. The long-term (FUV-MUV) color reconstruction is introduced in Section 2. Two datasets are used to reconstruct it: the Sunspot Number (SSN) and the solar Ca II K index. This reconstruction allows us to estimate solar color variations (FUV-MUV) in the past without the use of SSI models. In Section 3, the long-term (FUV-MUV) color reconstruction is applied to estimate area coverage of solar magnetic features (i.e., faculae). In order to test the performance of our method and validate it for the solar case we compare our area coverages and coverages obtained from historical full-disk observations. In Section 4, Ca II K and Mg II indices are reconstructed using a semi-empirical approach. Our reconstructions are compared with available observations/reconstructions and extended in the past until 1749. The main results are summarized in Section 5.

2. Long-term (FUV-MUV) Color Reconstruction

Basically, all our knowledge about past solar magnetic activity rests on the use of spatially resolved maps of solar surface (e.g., continuum images at different wavelengths, photo-

spheric magnetograms, full-disk Ca II K spectro-heliograms), sunspot related benchmarks (e.g., Sunspot Number, Group Sunspot Number, sunspot area), or indirect and Sun-as-a-star solar proxies (e.g., concentrations of cosmogenic isotopes, Mg II index, Ca II K index, radio flux at 10.7 cm).

The solar irradiance reconstructions based on spatially resolved maps of solar surface, available from a few dozens of years, are the result of sophisticated models that use the techniques of segmentation of solar magnetic structures, e.g., sunspot, faculae, network, quiet Sun, etc., based on single maps or on the combined use of these (e.g. Muscheler *et al.*, 2016). Techniques of segmentation and recognition of photospheric and chromospheric structures, mainly devoted to the study of irradiance variations associated to quiet network and topology of solar convective structures, have been used by our team for more than 20 years (e.g. Berrilli, Florio, and Ermolli, 1998; Berrilli *et al.*, 1999, 2002; Ermolli, Berrilli, and Florio, 2003; Berrilli *et al.*, 2004, 2005a,b; Goldbaum *et al.*, 2009; Forte *et al.*, 2018). Clearly, these techniques cannot be applied to the Sun before the availability of solar images or full-disk Ca II K spectro-heliograms or to investigate stars not spatially resolved.

On the other hand, sunspots and indirect Sun-as-a-star solar proxies, as the Ca II K and Mg II indices or concentrations of cosmogenic isotopes, allow us to investigate the solar behavior back in time (time scales of decades or centuries) and can potentially be applied to stars not spatially resolved, for example to parental stars hosting extra-solar planets.

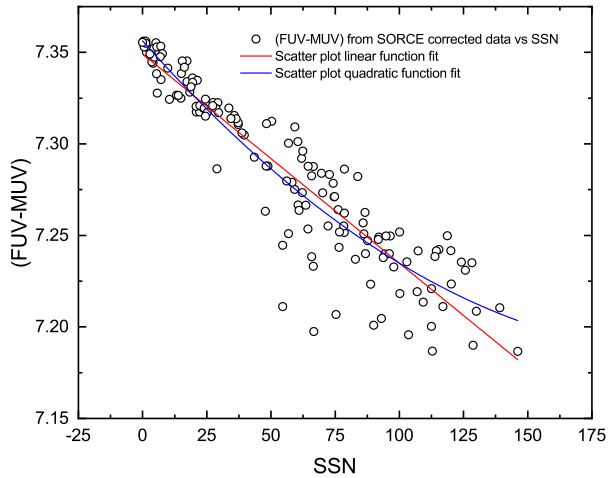
One may notice that the use of proxies based on concentrations of cosmogenic isotopes, created by the interaction of galactic cosmic rays with Earth's atmosphere and modulated by the solar "open" field (e.g. Wu *et al.*, 2018), allow us to guess the solar magnetic activity on the scale of millennia. Nevertheless, the geographical origin of the cosmogenic isotopes, the Earth's climate and atmospheric dynamics, and the variability of the Earth's magnetic field remain major issues of these methods (e.g. Muscheler *et al.*, 2016) especially when they extend in the past over geomagnetic secular variation timescales. As regard observations of sunspots, these are available for the past four centuries since Galilei demonstrated their association to the Sun in 1613. The solar (FUV-MUV) color is a UV solar spectral proxy introduced by Lovric *et al.* (2017) to describe the ratio of fluxes in two different spectral regions of the UV spectral energy distribution of the Sun, nominally the FUV (115–180 nm) and MUV (180–320 nm) SORCE SOLTICE bands. Consequently, this color is a measure of the solar spectral slope in the UV spectral region which is able, as discussed in Section 1, to alter the chemical and physical processes in the Earth's upper atmosphere. The color is calculated using the equation:

$$(\text{FUV} - \text{MUV}) = -2.5 \log \frac{F_{\text{FUV}}}{F_{\text{MUV}}}, \quad (1)$$

where (FUV-MUV) is the color in magnitudes and F_{FUV} and F_{MUV} are the integrated fluxes of SORCE SOLTICE instruments (McClintock, Snow, and Woods, 2005; McClintock, Rottman, and Woods, 2005). It is worth noting that, in the color formula the magnitude zero-points are arbitrarily set to zero corresponding to a simple offset in the color, i.e., a vertical shift by a constant amount. More details about (FUV-MUV) color and aging correction to SORCE data can be found in Lovric *et al.* (2017) and Criscuoli *et al.* (2018).

The correlation of the (FUV-MUV) color and the Mg II core-to-wing index was investigated in Criscuoli *et al.* (2018). Because Mg II systematic measurements are available only from the late-1970s, here we investigate whether such strong correlation holds also for the Ca II K index and the sunspot number (SSN), measurements of such proxies dating back to several decades. To this aim we analyzed the following datasets: the (FUV-MUV) color, estimated from SORCE measurements after aging was removed (Lovric *et al.*, 2017); the

Figure 1 The (FUV-MUV) vs SSN relation for the linear (red line) and quadratic (blue line) fits. The adopted linear function is $(FUV - MUV) = -0.00114 \times SSN + 7.35$.



Ca II K Emission index time series from the National Solar Observatory, which dates back to 1907;² the SILSO monthly mean SSN data from 1749.³

The relation between the variability of the (FUV-MUV) color with the SSN is illustrated in Figure 1. Two fits, i.e., linear and quadratic functions, were performed on (FUV-MUV) vs SSN data. We decided to use the linear fit (the R^2 values for the two fits are similar) mainly for two reasons: i) for the sake of simplicity; ii) the weakness of the last Solar Cycle 24 prevented us from extending the correlation analysis to high SSN values. This affected the estimation of the quadratic function parameters and, particularly, the evaluation of the deviation from linearity for high SSN values. Indeed, assuming the parameters obtained from a quadratic fit, saturation effects on the reconstruction of the facular coverage appear.

The correlation between (FUV-MUV) and Ca II K index shows a similar behavior as (FUV-MUV) and Mg II index. This correlation is not shown here because of space limitation. Also in this case we fitted the data using both a linear and a quadratic function and a linear correlation was assumed. The correlation is

$$(FUV - MUV) = -18.31 \text{ Ca II K index} + 8.856 \tag{2}$$

and is used to estimate the UV color prior to 2003, when SOLSTICE observations started.

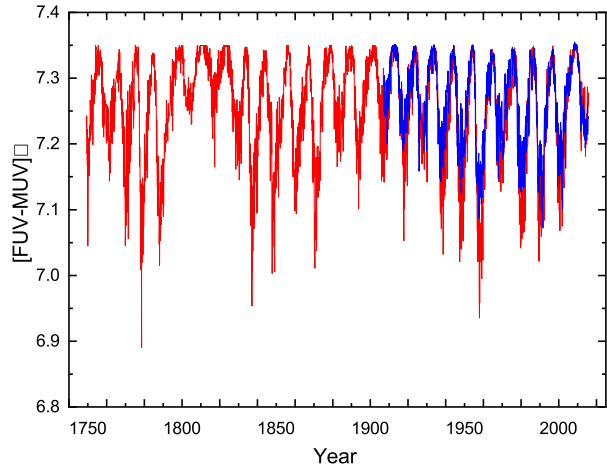
The reconstructed monthly average (FUV-MUV) color long-term variations, using the SSN and the Ca II K correlations, are shown in Figure 2. Both (FUV-MUV) reconstructions show very similar trends, i.e., the (FUV-MUV) color decreases as the solar activity increases. It is important to remember here that a lower (FUV-MUV) means a greater FUV flux increase in comparison to MUV flux, i.e., as the Sun’s magnetic activity increases, the color index (FUV-MUV) becomes lower.

In order to quantify the similarity between the two reconstructions, a correlation measure has been carried out. We performed a linear regression between long-term (FUV-MUV) reconstructions, in the time interval in which SSN and Ca II K index overlap, and we obtained a Pearson correlation coefficient equal to 0.86 and a slope equal to 1.15, considering (FUV-MUV) reconstructed using SSN as the dependent variable. The slope different from one tells

²The NSO Ca II K emission index is available at: <http://gong.nso.edu/data/magmap>.

³The World Data Center SILSO (Sunspot Index and Long-term Solar Observations), Royal Observatory of Belgium, Brussels, data can be found at: <http://sidc.be/silso/datafiles>.

Figure 2 (FUV-MUV) color index monthly mean reconstruction from SSN (red line) and Ca II K index (blue line). The reconstructions are based on linear correlations between observed (FUV-MUV) color and SSN and Ca II K index, respectively.



us that (FUV-MUV) has a different sensitivity to a physical proxy like Ca II K (this line was advocated as proxy for the FUV by Lean *et al.*, 1982) respect to an arbitrary activity proxy as the SSN. Nonetheless, in Section 2, given the wider temporal coverage of SSN compared to Ca II K, we will use the correlation between the (FUV-MUV) color and SSN in order to reconstruct solar magnetic feature coverages.

3. Long-term Reconstruction of Solar Magnetic Feature Coverage

In order to validate the use of broad-band colors, as (FUV-MUV), to investigate stellar and solar variability, we compare solar magnetic feature coverage reconstructions, derived from (FUV-MUV) reconstructions shown in Section 2, against “state-of-the-art” coverage datasets. More in detail, we describe how, making use of (FUV-MUV) color, we derive the area coverage of solar magnetic features (i.e., area of sunspots, faculae and network) at times when direct observations were not available. These, in turn, are employed to estimate long-term variability of the Ca II K and Mg II indices, following the procedure described in Section 4.

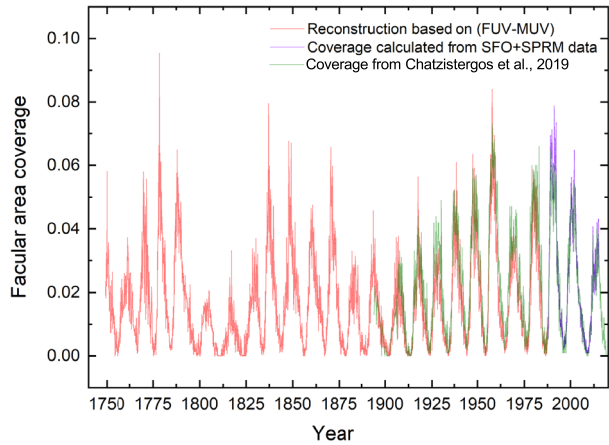
3.1. Estimate of Facular Area Coverage

Our reconstruction of the area coverage of faculae is based on the empirical long-term reconstruction of (FUV-MUV) color shown in Section 2. The assumption is that variability of UV radiation is mostly modulated by the facular contribution (e.g. Shapiro *et al.*, 2016). The UV irradiance can be therefore reconstructed by taking into account only quiet Sun and facular contribution. In this way, we can write the (FUV-MUV) color as:

$$(FUV - MUV) = -2.5 \log\left(\frac{F_{FUV}}{F_{MUV}}\right) = -2.5 \log\left(\frac{\alpha_f F_{FUV}^f + (1 - \alpha_f) F_{FUV}^q}{\alpha_f F_{MUV}^f + (1 - \alpha_f) F_{MUV}^q}\right) \quad (3)$$

where the superscript symbols f and q indicate the facular and the quiet Sun contributions to F_{FUV} and F_{MUV} fluxes, respectively. Through simple algebraic manipulation, we can rewrite

Figure 3 The reconstruction of facular area coverage through: (MUV-FUV) color (red line) and composed coverage from SFO and SPRM (violet line). For comparison the composite of plage area of Chatzistergos *et al.*, 2019 is shown (olive line).



this equations as

$$\frac{1 + \alpha_f \delta_{FUV}}{1 + \alpha_f \delta_{MUV}} = 10^{2(C_q - C)/5} \tag{4}$$

where δ_{MUV} and δ_{FUV} are the relative facular contrast in the MUV and FUV range, respectively, and C and C_q are the (FUV-MUV) color derived from the SSN and quiet Sun, respectively. C_q , δ_{MUV} and δ_{FUV} are synthetically computed by using the models 1001 and 1005 of the set of seven semi-empirical atmosphere models from the Solar Irradiance Physical Modeling (SRPM) system described in Fontenla *et al.* (2011).

By solving Equation 4 for α_f , we obtain

$$\alpha_f = \frac{10^{2(C_q - C)/5} - 1}{\delta_{FUV} - 10^{2(C_q - C)/5} \delta_{MUV}} \tag{5}$$

The synthetic reconstruction was performed using the procedure described in detail in Criscuoli *et al.* (2018).

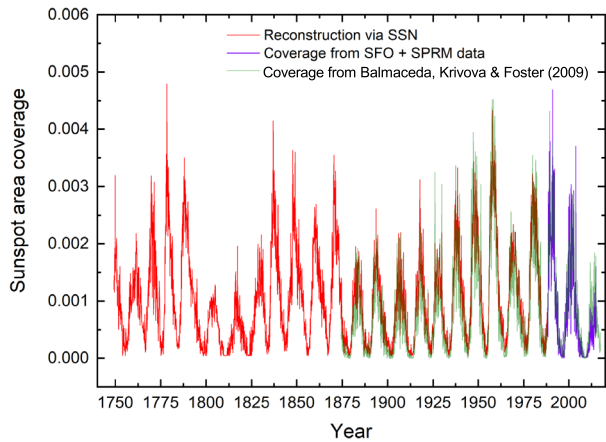
Eventually, the (FUV-MUV) color long-term variation has been reconstructed for the period 1749–2015. The reconstruction is split into two periods. For the period 1988–2015 we employed the semi-empirical approach described in Criscuoli *et al.* (2018) making use of the facular coverage calculated by means of segmentation techniques of solar full-disk images. More in detail, we used for the period 1988–2003 the facular area coverage obtained from San Fernando Observatory data (Walton, Preminger, and Chapman, 2003; Preminger and Walton, 2006) and for the period 2003–2015 the facular area coverage obtained from the Precision Solar Photometric Telescope data (PSPT Rast *et al.*, 1999) by using the SRPM system (Fontenla *et al.*, 2011; Fontenla and Harder, 2005).⁴ For the period 1749–1987 we used the (FUV-MUV) color reconstructed using the SSN, as described in Section 2.

The facular area reconstructed for the period from 1749 to 1987 is illustrated in Figure 3. For comparison, we show the area coverage from 1988 to 2015 derived from San Fernando Observatory (SFO) and Precision Solar Photometric Telescope (PSPT) observations, and the *plage* composite from 1893 to 2015 derived from historical archives of full-disk Ca II K observations (Chatzistergos *et al.*, 2019).⁵ The regression analysis between our reconstructed

⁴The facular area coverage obtained from the PSPT are available at: http://lasp.colorado.edu/pspt_access.

⁵The *plage* composite from 1893 to 2015 is available at: <http://www2.mps.mpg.de/projects/sun-climate/data>.

Figure 4 Sunspot area coverage reconstructed from SSN (red line) compared with spot area coverage from SFO and SRPM (violet line). For comparison, the plot shows the sunspot area composite (olive line) by Balmaceda *et al.* (2009).



facular area coverage and the composite (Chatzistergos *et al.*, 2019) of plages, the chromospheric counterpart of faculae, over the period 1893–2015 produces a Pearson correlation coefficient of 0.94 pointing out the strong correlation between the two reconstructions.

3.2. Estimate of Sunspot and Network Area Coverage

The temporal variation of sunspot area coverage can be estimated using the SSN (e.g. Wilson and Hathaway, 2006; Tapping and Morgan, 2017). In this study we used a power-law model to derive sunspot area coverage α_s from SSN:

$$\alpha_s = a \text{SSN}^b \quad (6)$$

where the a and b parameters are assumed constant with time. A parameter fitting performed over the entire set of SFO and PSPT observations provided $a = 1.246 \times 10^{-6}$ and $b = 1.418$. The calculated sunspot coverage does not consider the difference between umbra and penumbra, basically because the ratio between them does not remain constant in time, as reported by different authors (e.g. Carrasco *et al.*, 2018; Jha, Mandal, and Banerjee, 2018). Figure 4 shows the sunspot area reconstructed using Equation 6 together with the area derived from SFO,⁶ and PSPT full-disk observations using the Solar Radiation Physical Modeling (SRPM) system.⁷ For comparison, the plot also shows the Sunspot area composite by Balmaceda *et al.* (2009)⁸ for the period 1874–2015, which was obtained after cross-calibration of measurements by different observers. As for the facular area, our estimated sunspot area and sunspot coverage estimated from full-disk observations (Balmaceda *et al.*, 2009) strongly correlate. We calculate a Pearson correlation coefficient of 0.93 between our reconstruction and the sunspot area composite by Balmaceda *et al.* (2009) over the period 1874–2015.

A similar approach is used to derive the network coverage. The employed empirical relation with SSN data is the following:

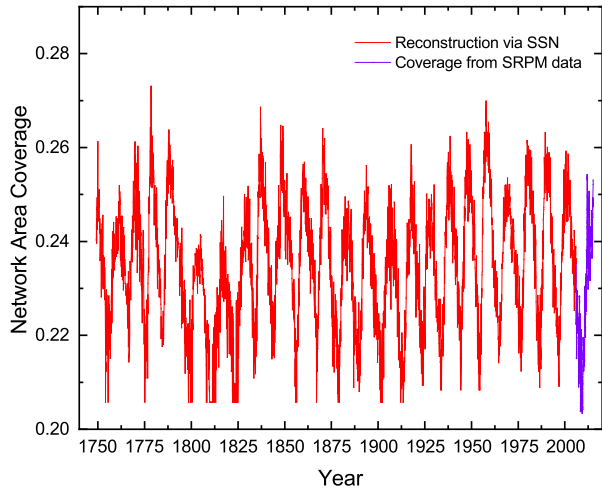
$$\alpha_n = d \text{SSN}^f + g \quad (7)$$

⁶The sunspot area is available at SFO, a solar research facility associated with the California State University: <http://www.csun.edu/SanFernandoObservatory/photoindex.html>.

⁷The SRPM model is available at: http://lasp.colorado.edu/pspt_access.

⁸The sunspot area composite is available at: <http://www2.mps.mpg.de/projects/sun-climate/data.html>.

Figure 5 The network area coverage (red solid line), estimated as explained in the text, together with the network area coverage derived from SRPM observations (violet solid line).



where the d , f and g parameters are assumed constant with time. Unfortunately, only the SRPM observations from 2005 are available to estimate the parameters of the above relation. The calculated fit is $d = 1.047 \times 10^{-3}$, $f = 0.712$ and $g = 0.212$. Figure 5 shows the reconstruction of network area coverage.

4. Reconstruction of Ca II K and Mg II Indices

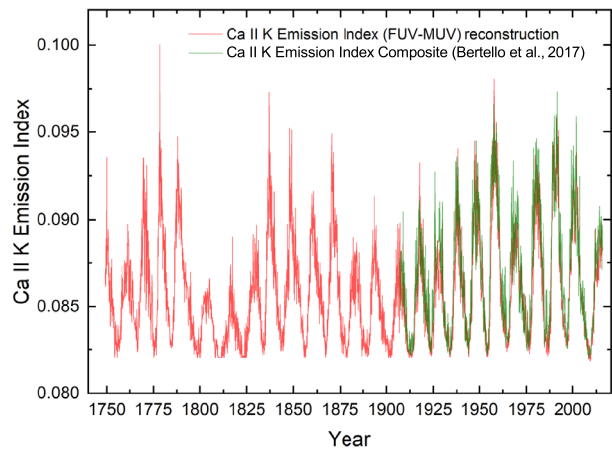
As reported in Bertello *et al.* (2016) long-term synoptic Ca II K observations constitute a fundamental database for a variety of historical analyses of the state of the solar magnetism. On the other hand, the composite Mg II index spanning from 1978 to present, constitutes a compelling proxy for spectral solar irradiance variability from the UV to EUV (e.g. Dudok de Wit *et al.*, 2009). The final test bench for our method consists therefore in reconstructing these two indices starting from 1749 and comparing our reconstructions, during the overlapping period, with the datasets obtained from analysis of full-disk historical images or direct measurements. Our reconstruction of the Ca II K and Mg II indices was performed using a semi-empirical approach, under the assumption that solar variability is modulated by the presence of magnetic features over the solar disk (e.g. Penza *et al.*, 2003; Penza, Pietropaolo, and Livingston, 2006; Ermolli, Criscuoli, and Giorgi, 2011; Fontenla *et al.*, 2011; Yeo, Krivova, and Solanki, 2014; Yeo *et al.*, 2017). As such, the solar spectral flux at any time t can be reproduced as the linear combination of synthetic fluxes $F_j(\lambda)$ representing quiet and magnetic regions (e.g. quiet, network, faculae and sunspot) weighed by the corresponding area coverage $\alpha_j(t)$:

$$F(\lambda, t) = \sum_j \alpha_j(t) F_j(\lambda). \tag{8}$$

By using the coverages obtained in the previous section we are able to reconstruct spectral indices from 1749 to 2015; in particular, we estimate the variations of the Ca II K emission and the Mg II core-to-wing indices.

As mentioned in Section 1, these indices are excellent proxies of both solar and stellar magnetic activity (e.g. Preminger, Chapman, and Cookson, 2011; Salabert *et al.*, 2016; Lee,

Figure 6 Ca II K Emission Index reconstructed as explained in the text (red line) compared with the NSO Ca II K index composite (olive line).



Cahalan, and Wu, 2018). Even in this case the procedure is similar to the one adopted in Criscuoli *et al.* (2018) for the reconstruction of the Mg II index. In particular, the synthetic fluxes were produced with the RH code (Uitenbroek, 2001) making use of the set of atmosphere models published in Fontenla *et al.* (2011). The synthesis of the Ca II 393 nm resonance line was performed in NLTE using a 6 levels model atom and PRD approximation. The synthesis of the Mg II H and K lines was performed in NLTE and PRD as well, as described in detail in Criscuoli *et al.* (2018). In both cases, background lines in the relevant spectral ranges were computed in LTE, using atomic and molecular parameters from the Kurucz website.⁹

The reconstructed Ca II K emission index is shown in Figure 6, together with the Ca II K emission index derived from Mount Wilson measurements (Bertello *et al.* (2016)) for the time these are available. The plot shows that the reconstructed and measured indices are in good agreement. In detail, the regression between our reconstruction and the Ca II K emission index derived from Mount Wilson measurements, over the period 1907–2015, produces a Pearson correlation coefficient of 0.88 with an average relative difference of 2%. This result suggests that our reconstruction provides a reasonable estimate for the period 1749–1902, when direct measurements were not available.

The reconstructed Mg II core-to-wing index is shown in Figure 7, together with the measured Bremen Mg II composite (Viereck *et al.*, 2004). The regression between the Mg II reconstruction and the Bremen Mg II composite, over the period 1978–2015, produces a Pearson correlation coefficient of 0.92 with an average relative difference of 1.6%.

Finally, Figure 8 shows the correlations between the reconstructed (FUV-MUV) color and Ca II K emission and Mg II indices. These correlations are very similar supporting the idea that (FUV-MUV) is essentially modulated by the facular emission, i.e. from the FUV flux.

5. Conclusions

The solar UV radiation originates in the layers of the atmosphere between the high photosphere and the corona. This radiation has a profound impact on the upper Earth's at-

⁹The Kurucz website is available at <http://kurucz.harvard.edu/>.

Figure 7 Comparison of Mg II index variations reconstructed with our model (red line) and the Bremen composite index (olive line).

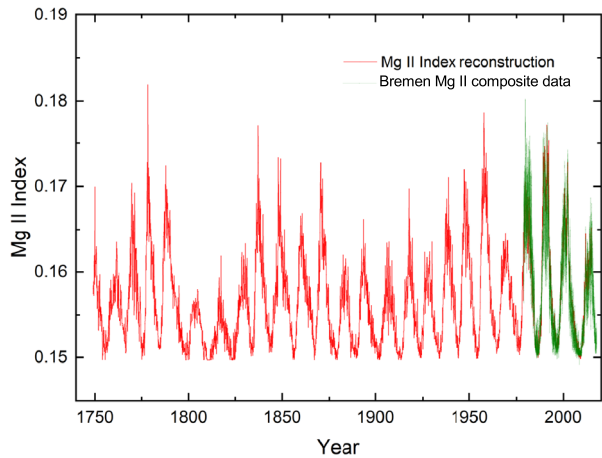
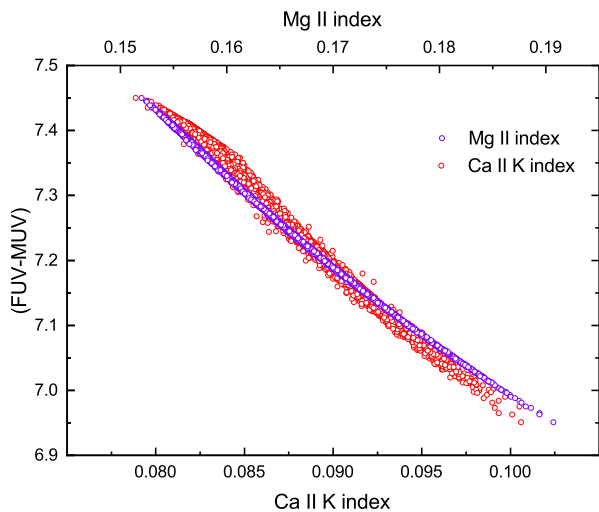


Figure 8 The correlation between (FUV-MUV) color and the Ca II K index (red open circles) and Mg II index (violet open circles) reproduced by our reconstructions. The curves are horizontally shifted for clarity.



mosphere, including the stratosphere and thermosphere. In particular stratospheric ozone, which might influence the thermal and dynamical structure of the middle terrestrial atmosphere and consequently the radiative forcing of the troposphere, is produced by the action of solar UV radiation on diatomic oxygen. The photochemical processes that lead to the dissociation of molecular oxygen and ozone require the presence of UV photons at different thresholds. As a consequence, the detail of the solar spectrum can be neglected in the first approximation, to estimate the stratospheric ozone production rates. Essentially for this reason we introduced a new spectral UV index based on the (FUV-MUV) color (Lovric *et al.*, 2017; Criscuoli *et al.*, 2018) calculated using SORCE SOLSTICE integrated fluxes in the FUV and MUV bands.

This paper presents the long-term (1749–2015) reconstruction of three UV proxies of solar variability, namely the (FUV-MUV) color, the Ca II k emission index and the Mg II core-to-wing ratio, by examining the long-term variability of solar activity. The SSN was the only proxy of the solar activity employed to estimate the variability of the solar UV indices since 1749.

The use of spectral indices that can be derived from observations of the Sun-as-a-star is very important for the study of Sun-like star activity, possibly host-stars of extra-solar planetary systems.

The agreement between the UV indices calculated with our approach and the composites obtained with state-of-the-art techniques, applied to full-disk observations, demonstrates that our approach has comparable utility for exploring the behavior of the Sun in the past, when it is no longer possible to use techniques based on full-disk images, and represents a useful tool in characterizing UV activity of stars that cannot be spatially resolved.

For completeness, we must note that our reconstructions, based on solar proxies associated with closed-field magnetic structures, e.g., sunspots, currently do not include possible large trend which can be deduced, for example, from the content of concentrations of cosmogenic isotopes (see Section 1 in this paper) modulated by open-field solar structures transiting through the corona and filling the whole heliosphere. This analysis will be introduced and discussed in a future paper, in preparation, focused on the reconstruction of long-term solar TSI.

Our main results are summarized as follows:

- i) The long-term variation of the (FUV-MUV) color was reconstructed for the period 1749–2015. The reconstruction is split in to two periods: *i*) the period 1988–2015, for which we employed a semi-empirical approach making use of the facular coverage calculated by means of segmentation techniques of solar full-disk images; *ii*) the period 1749–1987, for which the (FUV-MUV) color was derived assuming a linear relation with the SSN.
- ii) The sunspot, faculae and network area coverage was reconstructed for the period 1749–2015. The area of faculae was estimated through the reconstructed (FUV-MUV) color index, while network and sunspot area were derived from the SSN. In all cases we find a very satisfactory agreement between the reconstructed area coverages and those obtained by the analysis of full-disk observations, at the times these are available.
- iii) By using the estimated area coverage of magnetic features, we were able to reconstruct the variability of the Ca II K emission index and of the Mg II core-to-wing ratio index from 1749 to 2015. In both cases, the reconstructions present a very satisfactory agreement with observations, at the times these are available. In this context, we demonstrate the ability of our approach, which makes use of a simplified treatment of solar magnetic structures, to reconstruct historical solar UV proxies at the times these are available.

Acknowledgements The National Solar Observatory is operated by the Association of Universities for Research in Astronomy, Inc. (AURA), under cooperative agreement with the National Science Foundation. The Time series of the Ca II K uses SOLIS data obtained by the NSO Integrated Synoptic Program (NISIP), managed by the National Solar Observatory, which is operated by the Association of Universities for Research in Astronomy (AURA), Inc. under a cooperative agreement with the National Science Foundation downloaded from the SOLIS website (<https://solis.nso.edu/0/iss/>). The following institutes are acknowledged for providing the data: Laboratory for Atmospheric and Space Physics (Boulder, CO) for SORCE SOLSTICE SSI data (<http://lasp.colorado.edu/home/sorce/data/>) and University of Bremen (Bremen, Germany) for Mg II index data (<http://www.iup.uni-bremen.de/gome/gomemgii.html>). This work was partially supported by Italian MIUR-PRIN grant 2017 “on Circumterrestrial Environment: Impact of Sun–Earth Interaction” and the Joint Research PhD Program in “Astronomy, Astrophysics and Space Science” between the universities of Roma Tor Vergata, Roma Sapienza and INAF.

Disclosure of Potential Conflicts of Interest The authors declare that they have no conflicts of interest.

Publisher's Note Springer Nature remains neutral with regard to jurisdictional claims in published maps and institutional affiliations.

References

- Balmaceda, L., Solanki, S.K., Krivova, N.A., Foster, S.: 2009, A homogeneous database of sunspot areas covering more than 130 years. *J. Geophys. Res.* **114**, A7. DOI. ADS.
- Berrilli, F., Florio, A., Ermolli, I.: 1998, On the geometrical properties of the chromospheric network. *Solar Phys.* **180**, 29. DOI. ADS.
- Berrilli, F., Ermolli, I., Florio, A., Pietropaolo, E.: 1999, Average properties and temporal variations of the geometry of solar network cells. *Astron. Astrophys.* **344**, 965. ADS.
- Berrilli, F., Consolini, G., Pietropaolo, E., Caccin, B., Penza, V., Lepreti, F.: 2002, 2-D multiline spectroscopy of the solar photosphere. *Astron. Astrophys.* **381**, 253. DOI. ADS.
- Berrilli, F., Del Moro, D., Consolini, G., Pietropaolo, E., Duvall, J.T.L., Kosovichev, A.G.: 2004, Structure properties of supergranulation and granulation. *Solar Phys.* **221**(1), 33. DOI. ADS.
- Berrilli, F., del Moro, D., Florio, A., Santillo, L.: 2005a, Segmentation of photospheric and chromospheric solar features. *Solar Phys.* **228**, 81. DOI. ADS.
- Berrilli, F., Del Moro, D., Russo, S., Consolini, G., Straus, T.: 2005b, Spatial clustering of photospheric structures. *Astrophys. J.* **632**(1), 677. DOI. ADS.
- Bertello, L., Pevtsov, A.A., Tlatov, A., Singh, J.: 2016, Solar Ca II K observations. *Asian J. Phys.* **25**, 295. ADS.
- Böhm-Vitense, E.: 2007, Chromospheric activity in G and K main-sequence stars, and what it tells us about stellar dynamos. *Astrophys. J.* **657**, 486. DOI. ADS.
- Bordi, I., Berrilli, F., Pietropaolo, E.: 2015, Long-term response of stratospheric ozone and temperature to solar variability. *Ann. Geophys.* **33**, 267. DOI. ADS.
- Carrasco, V.M.S., García-Romero, J.M., Vaquero, J.M., Rodríguez, P.G., Foukal, P., Gallego, M.C., Lefèvre, L.: 2018, The umbra-penumbra area ratio of sunspots during the Maunder Minimum. *Astrophys. J.* **865**, 88. DOI. ADS.
- Chapman, S.: 1932, Discussion of memoirs. On a theory of upper-atmospheric ozone. *Q. J. Roy. Meteorol. Soc.* **58**, 11. DOI. ADS.
- Chatterjee, S., Banerjee, D., McIntosh, S.W., Leamon, R.J., Dikpati, M., Srivastava, A.K., Bertello, L.: 2019, Signature of extended solar cycles as detected from Ca II K synoptic maps of Kodaikanal and Mount Wilson Observatory. *Astrophys. J. Lett.* **874**, L4. DOI. ADS.
- Chatzistergos, T., Ermolli, I., Krivova, N.A., Solanki, S.K.: 2019, Analysis of full disc Ca II K spectroheliograms II. Towards an accurate assessment of long-term variations in plage areas. *Astron. Astrophys.* **625**, 22. DOI.
- Criscuoli, S., Penza, V., Lovric, M., Berrilli, F.: 2018, The correlation of synthetic UV color versus Mg II index along the solar cycle. *Astrophys. J.* **865**, 22. DOI. ADS.
- Dudok de Wit, T., Kretzschmar, M., Liliensten, J., Woods, T.: 2009, Finding the best proxies for the solar UV irradiance. *Geophys. Res. Lett.* **36**(10), L10107. DOI. ADS.
- Egeland, R., Soon, W., Baliunas, S., Hall, J.C., Pevtsov, A.A., Bertello, L.: 2017, The Mount Wilson Observatory S-index of the Sun. *Astrophys. J.* **835**, 25. DOI. ADS.
- Ermolli, I., Berrilli, F., Florio, A.: 2003, A measure of the network radiative properties over the solar activity cycle. *Astron. Astrophys.* **412**, 857. DOI. ADS.
- Ermolli, I., Criscuoli, S., Giorgi, F.: 2011, Recent results from optical synoptic observations of the solar atmosphere with ground-based instruments. *Contrib. Astron. Obs. Skaln. Pleso* **41**, 73. ADS.
- Ermolli, I., Criscuoli, S., Uitenbroek, H., Giorgi, F., Rast, M.P., Solanki, S.K.: 2010, Radiative emission of solar features in the Ca II K line: comparison of measurements and models. *Astron. Astrophys.* **523**, A55. DOI. ADS.
- Fontenla, J., Harder, G.: 2005, Physical modeling of spectral irradiance variations. *Mem. Soc. Astron. Ital.* **76**, 826. ADS.
- Fontenla, J.M., Harder, J., Livingston, W., Snow, M., Woods, T.: 2011, High-resolution solar spectral irradiance from extreme ultraviolet to far infrared. *J. Geophys. Res., Atmos.* **116**, D20108. DOI. ADS.
- Forte, R., Jefferies, S.M., Berrilli, F., Del Moro, D., Fleck, B., Giovannelli, L., Murphy, N., Pietropaolo, E., Rodgers, W.: 2018, The MOTH II Doppler-magnetographs and data calibration pipeline. In: Foullon, C., Malandraki, O.E. (eds.) *Space Weather of the Heliosphere: Processes and Forecasts, IAU Symposium* **335**, 335. DOI. ADS.
- Goldbaum, N., Rast, M.P., Ermolli, I., Sands, J.S., Berrilli, F.: 2009, The intensity profile of the solar supergranulation. *Astrophys. J.* **707**, 67. DOI. ADS.
- Haigh, J.D.: 2003, The effects of solar variability on the Earth's climate. *Phil. Trans. Roy. Soc. London Ser. A* **361**, 95. DOI. ADS.
- Hall, J.C., Lockwood, G.W.: 1998, The solar activity cycle. I. Observations of the end of cycle 22, 1993 September–1997 February. *Astrophys. J.* **493**, 494. DOI. ADS.

- Jha, B.K., Mandal, S., Banerjee, D.: 2018, Long-term variation of sunspot penumbra to umbra area ratio. In: Banerjee, D., Jiang, J., Kusano, K., Solanki, S. (eds.): *IAU Symposium* **340**, 185. DOI. ADS.
- Jungclaus, J.H., Bard, E., Baroni, M., Braconnot, P., Cao, J., Chini, L.P., Egorova, T., Evans, M., Fidel González-Rouco, J., Goosse, H., Hurr, G.C., Joos, F., Kaplan, J.O., Khodri, M., Klein Goldewijk, K., Krivova, N., LeGrande, A.N., Lorenz, S.J., Luterbacher, J., Man, W., Maycock, A.C., Meinshausen, M., Moberg, A., Muscheler, R., Nehrbass-Ahles, C., Otto-Bliesner, B.I., Phipps, S.J., Pongratz, J., Rozanov, E., Schmidt, G.A., Schmidt, H., Schmutz, W., Schurer, A., Shapiro, A.I., Sigl, M., Smerdon, J.E., Solanki, S.K., Timmreck, C., Toohey, M., Usoskin, I.G., Wagner, S., Wu, C.-J., Leng Yeo, K., Zanchettin, D., Zhang, Q., Zorita, E.: 2017, The PMIP4 contribution to CMIP6—Part 3: The last millennium, scientific objective, and experimental design for the PMIP4 past1000 simulations. *Geosci. Model Dev.* **10**, 4005. DOI. ADS.
- Kaltenegger, L.: 2017, How to characterize habitable worlds and signs of life. *Annu. Rev. Astron. Astrophys.* **55**, 433. DOI. ADS.
- Lean, J.: 2000, Evolution of the Sun's spectral irradiance since the Maunder Minimum. *Geophys. Res. Lett.* **27**, 2425. DOI. ADS.
- Lean, J.: 2017, Sun–Climate connections. Oxford Research Encyclopedia. DOI.
- Lean, J.L., White, O.R., Livingston, W.C., Heath, D.F., Donnelly, R.F., Skumanich, A.: 1982, A three-component model of the variability of the solar ultraviolet flux 145–200 nm. *J. Geophys. Res.* **87**, 10307. DOI. ADS.
- Lee, J.N., Cahalan, R.F., Wu, D.L.: 2018, Solar rotational modulations of spectral irradiance and correlations with the variability of solar proxies. *Geophys. Res. Abstr.* **20**, A33.
- Linsky, J.: 2014, The radiation environment of exoplanet atmospheres. *Challenges* **5**, 351. DOI. ADS.
- Linsky, J.L.: 2017, Stellar model chromospheres and spectroscopic diagnostics. *Annu. Rev. Astron. Astrophys.* **55**, 159. DOI. ADS.
- Lovric, M., Tosone, F., Pietropaolo, E., Del Moro, D., Giovannelli, L., Cagnazzo, C., Berrilli, F.: 2017, The dependence of the [FUV-MUV] colour on solar cycle. *J. Space Weather Space Clim.* **7**(27), A6. DOI. ADS.
- McClintock, W.E., Rottman, G.J., Woods, T.N.: 2005, Solar-stellar irradiance comparison experiment II (SOLSTICE II): Instrument concept and design. *Solar Phys.* **230**(1–2), 225. DOI. ADS.
- McClintock, W.E., Snow, M., Woods, T.N.: 2005, Solar-stellar irradiance comparison experiment II (SOLSTICE II): Pre-launch and on-orbit calibrations. *Solar Phys.* **230**(1–2), 259. DOI. ADS.
- Muscheler, R., Adolphi, F., Herbst, K., Nilsson, A.: 2016, The revised sunspot record in comparison to cosmogenic radionuclide-based solar activity reconstructions. *Solar Phys.* **291**(9–10), 3025. DOI. ADS.
- Penza, V., Pietropaolo, E., Livingston, W.: 2006, Modeling the cyclic modulation of photospheric lines. *Astron. Astrophys.* **454**, 349. DOI. ADS.
- Penza, V., Caccin, B., Ermolli, I., Centrone, M., Gomez, M.T.: 2003, Modeling solar irradiance variations through PSPT images and semiempirical models. In: Wilson, A. (ed.) *Solar Variability as an Input to the Earth's Environment, ESA Special Publication* **535**, 299. ADS.
- Pevtsov, A.A., Virtanen, I., Mursula, K., Tlatov, A., Bertello, L.: 2016, Reconstructing solar magnetic fields from historical observations. I. Renormalized Ca K spectroheliograms and pseudo-magnetograms. *Astron. Astrophys.* **585**, A40. DOI. ADS.
- Preminger, D.G., Walton, S.R.: 2006, Modeling solar spectral irradiance and total magnetic flux using sunspot areas. *Solar Phys.* **235**(1–2), 387. DOI. ADS.
- Preminger, D.G., Chapman, G.A., Cookson, A.M.: 2011, Activity-brightness correlations for the Sun and sun-like stars. *Astrophys. J. Lett.* **739**(2), L45. DOI. ADS.
- Rast, M.P., Fox, P.A., Lin, H., Lites, B.W., Meisner, R.W., White, O.R.: 1999, Bright rings around sunspots. *Nature* **401**, 678. DOI. ADS.
- Saar, S.H., Brandenburg, A.: 1999, Time evolution of the magnetic activity cycle period. II. Results for an expanded stellar sample. *Astrophys. J.* **524**, 295. DOI. ADS.
- Salabert, D., García, R.A., Beck, P.G., Egeland, R., Pallé, P.L., Mathur, S., Metcalfe, T.S., do Nascimento, J.-D. Jr., Ceillier, T., Andersen, M.F., Triviño Hage, A.: 2016, Photospheric and chromospheric magnetic activity of seismic solar analogs. Observational inputs on the solar-stellar connection from Kepler and Hermes. *Astron. Astrophys.* **596**, A31. DOI. ADS.
- Seppälä, A., Matthes, K., Randall, C.E., Mironova, I.A.: 2014, What is the solar influence on climate? Overview of activities during CAWSES-II. *Prog. Earth Planet. Sci.* **1**, 24. DOI. ADS.
- Shapiro, A.I., Solanki, S.K., Krivova, N.A., Yeo, K.L., Schmutz, W.K.: 2016, Are solar brightness variations faculae- or spot-dominated? *Astron. Astrophys.* **589**, A46. DOI. ADS.
- Tapping, K., Morgan, C.: 2017, Changing relationships between sunspot number, total sunspot area and F_{10.7} in Cycles 23 and 24. *Solar Phys.* **292**, 73. DOI.

- Tian, F., France, K., Linsky, J.L., Mauas, P.J.D., Vieytes, M.C.: 2014, High stellar FUV/NUV ratio and oxygen contents in the atmospheres of potentially habitable planets. *Earth Planet. Sci. Lett.* **385**, 22. [DOI](#). [ADS](#).
- Uitenbroek, H.: 2001, Multilevel radiative transfer with partial frequency redistribution. *Astrophys. J.* **557**, 389. [DOI](#). [ADS](#).
- Viereck, R.A., Floyd, L.E., Crane, P.C., Woods, T.N., Knapp, B.G., Rottman, G., Weber, M., Puga, L.C., DeLand, M.T.: 2004, A composite Mg II index spanning from 1978 to 2003. *Space Weather* **2**, S10005. [DOI](#). [ADS](#).
- Walton, S.R., Preminger, D.G., Chapman, G.A.: 2003, The contribution of faculae and network to long-term changes in the total solar irradiance. *Astrophys. J.* **590**(2), 1088. [DOI](#). [ADS](#).
- Warnecke, J.: 2018, Dynamo cycles in global convection simulations of solar-like stars. *Astron. Astrophys.* **616**, A72. [DOI](#). [ADS](#).
- Wilson, O.C.: 1978, Chromospheric variations in main-sequence stars. *Astrophys. J.* **226**, 379. [DOI](#). [ADS](#).
- Wilson, R.M., Hathaway, D.H.: 2006, On the Relation Between Sunspot Area and Sunspot Number. Technical report. [ADS](#).
- Wu, C.-J., Krivova, N.A., Solanki, S.K., Usoskin, I.G.: 2018, Solar total and spectral irradiance reconstruction over the last 9000 years. *Astron. Astrophys.* **620**, A120. [DOI](#). [ADS](#).
- Yeo, K.L., Krivova, N.A., Solanki, S.K.: 2014, Solar cycle variation in solar irradiance. *Space Sci. Rev.* **186**, 137. [DOI](#). [ADS](#).
- Yeo, K.L., Krivova, N.A., Solanki, S.K.: 2017, EMPIRE: a robust empirical reconstruction of solar irradiance variability. *J. Geophys. Res.* **122**(4), 3888. [DOI](#). [ADS](#).
- Yeo, K.L., Solanki, S.K., Norris, C.M., Beeck, B., Unruh, Y.C., Krivova, N.A.: 2017, Solar irradiance variability is caused by the magnetic activity on the solar surface. *Phys. Rev. Lett.* **119**, 091102. [DOI](#). [ADS](#).